Bulletin of the Seismological Society of America, Vol. 76, No. 5, pp. 1393–1405, October 1986

# COMPLEX POLARIZATION ANALYSIS OF PARTICLE MOTION

BY JOHN E. VIDALE

## ABSTRACT

**Knowledge of particle motion polarization aids in identifying phases on three-component seismograms. The scheme of Montalbetti and Kanasewich (1970) is extended to analytic three-component seismograms, where the imaginary part of the signal is the Hilbert transform of the real part. This scheme has only one free parameter, the length of the time window over which the polarization parameters are estimated, so it can be applied in a routine way to three-component data. The azimuth and dip of the direction of maximum polarization and the degree of elliptical polarization as a function of time for the seismograms are obtained.**

**Polarization analysis of strong motion data from the 1971 San Fernando earthquake aids in the discrimination between wave types, which is important for the understanding of the complicated earthquake-induced shaking observed in basins. Most arrivals are incident on the receivers in the direction of the back-azimuth to the epicenter, which suggests that despite the complicated motions, two-dimensional finite difference methods are sufficient to understand the effect on seismic waves of the Los Angeles and San Fernando basins (Vidale and Helmberger, 1986b).**

## INTRODUCTION

Although three-component seismograms are commonly used in many branches of seismology, the polarization content is analyzed only crudely and qualitatively. It is well known that $P$ waves, $S$ waves, Rayleigh waves, and Love waves have distinct polarization patterns (c.f. Aki and Richards, 1980; Gal'perin, 1984). One difficulty is that when more than one type of energy arrives in a record at the same time, it is hard to recover polarization data on either arrival, let alone both of them. Another problem is the conversion between $P$ and $S$ waves that takes place at the free surface for $P$-$SV$ energy, which may lead to phase differences between different components of motion for incident $SV$ waves (Nuttli, 1961) and Rayleigh surface waves (Aki and Richards, 1980). The proposed method identifies the problem of multiple arrivals by indicating a low degree of polarization and can handle elliptical polarization by the use of the analytic signal.

If structure is primarily laterally homogeneous, the Love wave appears mostly on the transverse component and the Rayleigh mostly on the vertical and radial components. Two-dimensional polarization analysis of the vertical and radial components can separate linearly polarized body waves from elliptically polarized Rayleigh waves, but will not help much with $SH$ body waves or Love waves. If structure is laterally heterogeneous, however, $P$-$SV$ and $SH$ energy will no longer cleanly separate onto the vertical and radial, and transverse components of ground motion, and a three-dimensional polarization analysis can aid in the identification and classification of arrivals in the seismogram. Anisotropic materials may also cause polarization anomalies (Kirkwood and Crampin, 1981), and such anomalies are easier to interpret with polarization analysis than by the traditional particle motion diagrams, which require visual interpretation.

## POLARIZATION ANALYSIS

A simple polarization analysis would consist of rotating the motion into the vertical, radial, and transverse components and inspecting them visually. One can

estimate the direction of polarization and perhaps, with some care and patience, determine whether the components are in phase for particular arrivals. The RE-MODE filter (Mims and Sax, 1965) and the polarization filter of Montalbetti and Kanasewich (1970) are used to enhance highly polarized portions of the signal automatically. The real counterpart to the filter described below was first presented by Montalbetti and Kanasewich (1970). Some theoretical considerations of polarization analysis are given in a series of papers by Samson and Olson (1980 and references therein) and Kanasewich (1981). A similar polarization filter designed to detect and determine the back-azimuth of events is described by Smart and Sproules (1981).

This scheme has only one free parameter, the length of the time window over which the polarization parameters are estimated, so it can be applied in a routine way to three-component data. The azimuth and dip of the direction of maximum polarization and the degree of elliptical polarization as a function of time for the seismograms are obtained.

## The Complex Polarization Filter

The data in polarization analysis is a three-component seismogram, that is, three time series, $\boldsymbol{u}_r(t)$ for the radial ($x$) component of motion, which is positive outward, $\boldsymbol{v}_r(t)$ for the tangential ($y$) component, which is positive in the clockwise direction, and $\boldsymbol{w}_r(t)$ for the vertical ($z$) component, which is positive upward. Each component is converted to an analytic signal

$$\boldsymbol{u}(t) = \boldsymbol{u}_r(t) + iH(\boldsymbol{u}_r(t)) \tag{1a}$$

$$\boldsymbol{v}(t) = \boldsymbol{v}_r(t) + iH(\boldsymbol{v}_r(t)) \tag{1b}$$

$$\boldsymbol{w}(t) = \boldsymbol{w}_r(t) + iH(\boldsymbol{w}_r(t)) \tag{1c}$$

where $H$ represents the Hilbert transform and $i$ is $\sqrt{-1}$.

The analytic signal may be used to compute the covariance matrix

$$\boldsymbol{C}(t) = \begin{bmatrix} \boldsymbol{uu}^* & \boldsymbol{uv}^* & \boldsymbol{uw}^* \\ \boldsymbol{vu}^* & \boldsymbol{vv}^* & \boldsymbol{vw}^* \\ \boldsymbol{wu}^* & \boldsymbol{wv}^* & \boldsymbol{ww}^* \end{bmatrix} \tag{2}$$

where the asterisks represent complex conjugation. The three eigenvalues $\lambda_i$ and eigenvectors $(x_i, y_i, z_i)$ of the 3 by 3 covariance matrix may be computed analytically (e.g., Malvern, 1969, p. 92) for each time point.

$$\begin{bmatrix} x_i \\ y_i \\ z_i \end{bmatrix} [\boldsymbol{C} - \lambda_i \boldsymbol{I}] = 0 \quad i = 1, 2, 3. \tag{3}$$

The analytic signal is complex, the covariance matrix is Hermitian and therefore has real positive eigenvalues, and the eigenvectors are in general complex.

The eigenvector $(x_0, y_0, z_0)$ associated with the largest eigenvalue $\lambda_0$ points in the direction of the largest amount of polarization. However, the phase in the complex plane of the eigenvectors is initially arbitrary. First, the eigenvector is normalized to have length 1. Then, by rotating the eigenvector associated with the largest eigenvalue by 0° to 180° in the complex plane, the rotation that results in the largest

real component may be found. This rotation may be found by searching over $\alpha = 0°$ to $180°$ to maximize $X$, the length of the real component of the eigenvector, where

$$X = \sqrt{(\mathrm{Re}(x_0 \mathrm{cis}\ \alpha))^2 + (\mathrm{Re}(y_0 \mathrm{cis}\ \alpha))^2 + (\mathrm{Re}(z_0 \mathrm{cis}\ \alpha))^2} \tag{4}$$

and cis $\alpha$ is $\cos \alpha + i \sin \alpha$ and $\mathrm{Re}(x)$ is the real part of $x$. The vector $(x_0, y_0, z_0)$ is then rotated by the angle $\alpha$, and the elliptical component of polarization may be estimated by

$$P_E = \frac{\sqrt{1 - X^2}}{X}. \tag{5}$$

Since the eigenvector is normalized, $\sqrt{1 - X^2}$ is the length of the complex part of the eigenvector, and $P_E$ is the ratio of the imaginary part of the eigenvector to the real part of the eigenvector. $P_E$ is 1 for circularly polarized motion, but $P_E$ is 0 for linearly polarized motion.

The sense of rotation may be found by comparing the signs of the real and imaginary parts of the rotated eigenvector. This information may be useful, for example, in resolving the ambiguity noted below for the direction of propagation for fundamental Rayleigh waves, which have retrograde polarization. An arbitrary mix of Rayleigh modes, however, could have either prograde, retrograde, or even linear polarization, so we pursue the sense of rotation no further in this paper. The dip of the polarization of Rayleigh waves also varies with the structure through which the Rayleigh wave is passing, but again not in a simple way.

The strike of the direction of maximum polarization is

$$\phi = \tan^{-1}\left(\frac{\mathrm{Re}(y_0)}{\mathrm{Re}(x_0)}\right). \tag{6}$$

Care must be exercised when $\mathrm{Re}(y_0)$ and $\mathrm{Re}(x_0)$ are small although $\mathrm{Im}(y_0)$ and $\mathrm{Im}(x_0)$ are not small, as would be the case for a Rayleigh wave when the direction of maximum polarization is nearly vertical. In that case, a different angle of rotation $\alpha$ may provide a more accurate estimation of the strike $\phi$.

The dip of the direction of maximum polarization is

$$\delta = \tan^{-1}\left(\frac{\mathrm{Re}(z_0)}{\sqrt{\mathrm{Re}(x_0)^2 + \mathrm{Re}(y_0)^2}}\right). \tag{7}$$

The polarization vector is ambiguous in that the vector $(x, y, z)$ represents the same polarization state as the vector $(-x, -y, -z)$. In this paper, the strike and dip defined in equations (6) and (7) range from $-90°$ to $90°$, where $0°$ strike and dip represents a vector which points horizontally in the direction back to the epicenter. The strikes $\phi$ in the range $-180°$ to $-90°$ and in the range $90°$ to $180°$ do not appear because of this ambiguity.

Similarly, the eigenvectors associated with the intermediate eigenvalue $\lambda_2$ and smallest eigenvalue $\lambda_1$ point in the directions of the intermediate and least amount of polarization, respectively. The eigenvectors corresponding to $\lambda_0$, $\lambda_1$, and $\lambda_2$ are

orthogonal, so only orthogonal components of polarization may be resolved. A measure of the strength of polarization in the signal is

$$P_S = 1 - \frac{\lambda_1 + \lambda_2}{\lambda_0}. \tag{8}$$

$P_S$ is near 1 if the signal is completely polarized in that there is only primarily one component of polarization, but $P_S$ is 0 if the largest component of polarization is only as big as the other two combined. A measure of the degree of planar polarization in the signal is

$$P_P = 1 - \frac{\lambda_1}{\lambda_2}. \tag{9}$$

$P_P$ is 1 if the intermediate component of polarization is much larger than the smallest component, but $P_P$ is near 0 if the intermediate and smallest components of polarization are comparable.

## Discussion

The use of the analytic, rather than just the real part of the signal has distinct advantages. The polarization can be measured from the covariance at any point in the seismogram, whereas with the real method, the covariance must be averaged over a portion of a wavelength before the polarization may be estimated. Also, the degree of ellipticity in the signal may be estimated. The only drawback is that four times the computation is required for the complex algebra.

Figure 1 shows the result of applying the polarization filter to synthetic waveforms. Figure 1, a through c, shows the seismograms that consist of a linearly polarized pulse followed by an elliptically polarized, longer period pulse. The correct values of $\phi$, $\delta$, and $P_E$ as a function of time are returned from the analysis and are shown in Figure 1, d to f. The transition between the two pulses is not abrupt in Figure 1, d to f, because the Hilbert transform has slightly averaged the polarization properties, mixing them in the region between the two pulses.

Simplification of the polarization method to two components rather than three is straightforward and can be useful in examining $P$-$SV$ motion. Figure 2, a and b, shows the result of applying polarization analysis to the vertical and radial velocity components of an elastic two-dimensional finite difference simulation (Vidale and Helmberger, 1986a). The source has a strike-slip mechanism, and the receiver is on the free surface at a range of eight source depths. The initial double pulse, which consists of direct $P$-wave energy and $S$-wave energy converted to $P$ on the free surface, has horizontal linear polarization, and the Rayleigh wave has vertical elliptical polarization. Figure 2, c and d, shows the dip of the polarization and a measure of the elliptical polarization estimated for each time point in the covariance matrix. Figure 2, e and f, shows the results when the covariance is averaged over 21 points and then analyzed for polarization. The averaged estimate is more stable but loses time resolution. By such an analysis, the Rayleigh polarization may be seen to tilt to the vertical as the receiver location becomes farther from the source.

This scheme differs from that of Montalbetti and Kanasewich (1970) in which a running average is subtracted from the seismograms before computing the covariance. This step is similar to high-pass filtering the data before polarization analysis.

If the data has a different frequency content than the background noise, then frequency filtering may improve the results of polarization analysis. In addition, and this is particularly true for the scheme of Montalbetti and Kanasewich (1970), the polarization character of the higher frequency energy is more stably estimated, as there are more wavelengths within the time-averaging window.

## Application to the San Fernando Earthquake

The San Fernando Earthquake of 1971 created numerous three-component ground motion records (Trifunac *et al.*, 1973). The strong motions recorded to the south of the event show the marked effects of the soft sediments that fill the San Fernando and Los Angeles basins. In another paper, we attempt to understand the

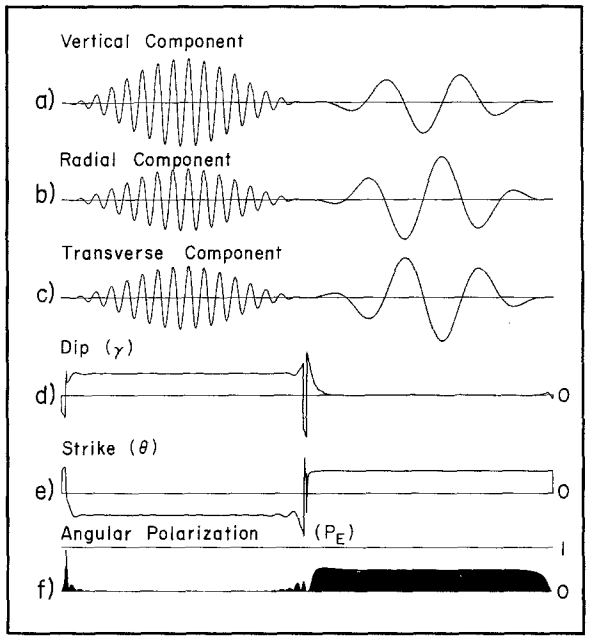


FIG. 1. Application of complex polarization filter to synthetic time series. The vertical, radial, and transverse components of the time series are shown in (a) to (c), respectively. (d) and (e) show the estimated dip and strike of the direction of maximum polarization, and (f) shows the degree of angular polarization as a function of time. The first half of the time series is linearly polarized, and the direction of maximum polarization has a strike of 45° and a dip of 45°. The second half of the time series is elliptically polarized, and the direction of maximum polarization has a strike of −45° and a dip of 0°. The complex polarization filter estimates the polarization parameters correctly in both cases.

effects of these basins on the strong ground motions by forward modeling with the finite-difference technique (Vidale and Helmberger, 1986b). In this section, we take the preliminary step of identifying phases in the three-component records with polarization analysis. This step is useful because not only the interpretation, but also the methods used to model the records depend on whether the motions are surface waves or body waves and to what extent the surface waves have been laterally refracted by structure.

Polarization analysis shows that the energy in the data is traveling mostly with a strike directly away from the epicenter, which indicates that out-of-plane arrivals are not important. This observation allows Vidale and Helmberger (1986b) to model the data using a finite difference scheme with structure that varies in the vertical

and radial directions, but not the transverse direction. The finite difference and polarization analyses both find that the surface waves that are converted from body waves at the edges of the basins are important.

Figure 3 shows relation between the epicenter of the San Fernando earthquake and the major basin structures. The profile $A$-$A'$ is the location of a cross-section compiled by Duke *et al.* (1971) which is summarized in the lower frame of Figure 3. The lower frame of Figure 3 shows the estimated location of the bottoms of the San Fernando and Los Angeles basins. Figure 4 shows the ground velocities recorded by

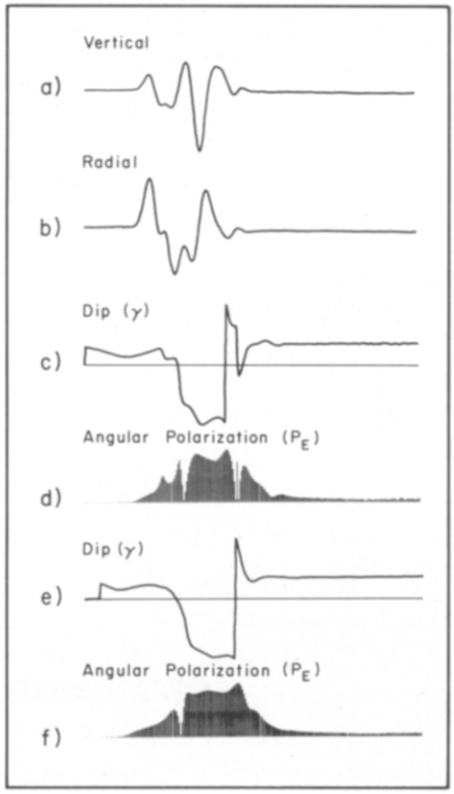


FIG. 2. Application of the two-dimensional complex polarization filter to seismograms generated by an elastic finite difference program. The source generates both compressional and shear waves, and is located in a half-space beneath a free surface. The receiver is on the free surface at a distance equivalent to eight source depths. (a) and (b) show the vertical and radial components of the displacement. (c) and (d) show polarization parameters estimated from using an averaging window one point wide. (e) and (f) show polarization parameters estimated from using an averaging window 21 points wide. Note the more stable estimates produced by using a longer time window.

the receivers that are marked by solid triangles in Figure 3. Note that the receivers are located in 4 areas: C041 is the Pacoima Dam station directly above the fault plane; C048, J145, and H115 are in the San Fernando basin; L166, D068, and D057 are on or near the Santa Monica Mountains; and S262, H118, S267, and N191 are in the Los Angeles basin. Figure 4 suggests that the mountains have a shorter duration of shaking than the basins, as has been noted previously for this profile (Liu and Heaton, 1984).

We will examine the records from stations J145, D068, and S267 in more detail with polarization analysis to investigate which paths the energy that shakes the basins follows. Figure 5 shows the result of polarization analysis of the velocity

records from station J145. A time-averaging window of 3 sec is used for Figures 5 through 7. Three arrivals have a clear polarization signature. The first arrival is mostly on the radial component and lasts 10 sec. It is apparently a direct $SV$ body wave. From the strike and dip of the direction of maximum polarization [$\theta$ and $\gamma$ defined in equations (6) and (7)], the arrival has horizontal polarization (e.g., the

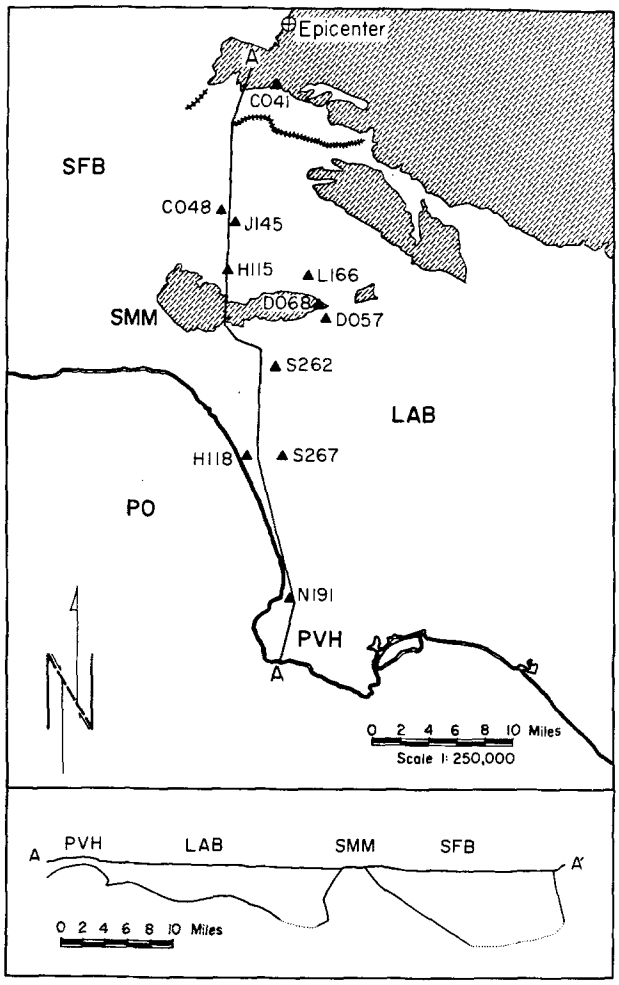


FIG. 3. Map and cross-section of the San Fernando region from Duke *et al.* (1971). The epicenter is marked by a cross. The filled triangles are the locations of the strong-motion instruments used in this section. *Cross-hatched area* shows surface exposure of bedrock. The bottom of the basins for the profile *A-A'* is shown below, with dashed portions showing where the boundary is not known. The cross-section has vertical exaggeration of 2:1. SFB locates the San Fernando basin, SMM the Santa Monica Mountains, LAB the Los Angeles basin, PVH the Palos Verdes hills, and PO the Pacific Ocean.

dip is near 0°) with an azimuth that is within 15° of the direction to the epicenter. From the low angular polarization [$P_E$ defined in equation (5)], we see that the arrival is linearly polarized. The high linear polarization [$P_S$ defined in equation (8)] shows that the largest component of polarization explains most of the observed covariance, so the polarization parameters of the arrival are reliably estimated.

The next arrival is a Love wave that shows a horizontal, linear polarization with an azimuth that is nearly transverse to the direction to the epicenter. An $SH$ body

wave would have the same polarization state as a Love wave, but is an unlikely interpretation of this phase due to its late arrival. The linear polarization, which is lower than for the first arrival, shows that there are large secondary components to the polarization, which may be seen in the nonnegligible energy on the vertical and radial components. The low linear polarization shows that the polarization parameters may not be reliably estimated. The third arrival is a Rayleigh wave, which is reliably estimated to be elliptically polarized on the radial and vertical components, although the strike may change significantly with time. Such shifts in azimuth of approach with time are also seen in array studies (Haar *et al.*, 1985).

The timing of this sequence with a shear body-wave arrival, followed by a Love wave, which is in turn followed by a Rayleigh wave, is not surprising. If the *SV*

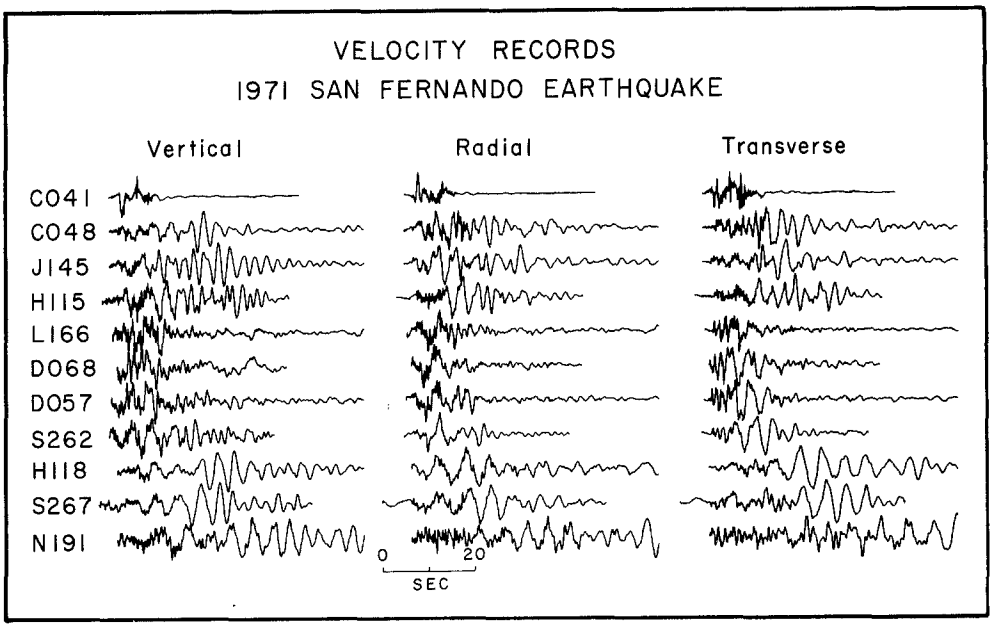


FIG. 4. Velocity records for the stations shown in Figure 3. The acceleration records are processed and integrated to yield velocity records as described by Trifunac *et al.* (1973). The horizontal components are rotated to radial and transverse components relative to the epicenter of the San Fernando earthquake. The traces are lined up to make a high-frequency arrival that is most evident on the vertical component arrive at the same time for all stations. The three-component station names are given to the left of the vertical component and the amplitudes in centimeters/sec are printed by each trace.

wave travels with a velocity of 3 km/sec, then the Love wave is traveling at 1.0 km/sec and the Rayleigh wave at 0.6 km/sec, which is reasonable since the near-surface *S*-wave velocity is about 0.6 km/sec (Duke *et al.*, 1971). The surface waves have not been significantly refracted laterally. The energy envelope is matched by the finite difference forward modeling (Vidale and Helmberger, 1986b).

The station D068, on the ridge, shows a more compressed sequence of arrivals in Figure 6 than does station J145 in Figure 5. The *S* body wave appears on both horizontal components, although primarily on the transverse component and is initially elliptically polarized, but in the horizontal plane. The Love wave, or perhaps another *SH* pulse, appears immediately after the *S* wave, and on the transverse component with good linear polarization. A suggestion of a Rayleigh wave is seen immediately following the Love wave as an increase in the ellipticity of the polarization. The short duration of the ground motion suggests that most of the energy on the ridge is from the body wave arrival.

The station S267 in the Los Angeles basin shows more unexpected behavior in Figure 7, with a Rayleigh wave arriving before a Love wave. The higher frequency energy that lasts 15 sec near the start of the record may be the $S$-wave arrival. It is reliably estimated. The next arrival is a Rayleigh wave. Although changing with time, the strike of the polarization of the arrival lines up with the back-azimuth to the epicenter, so the Rayleigh wave is propagating in the expected direction. The third arrival is a Love wave, again propagating near the expected azimuth.

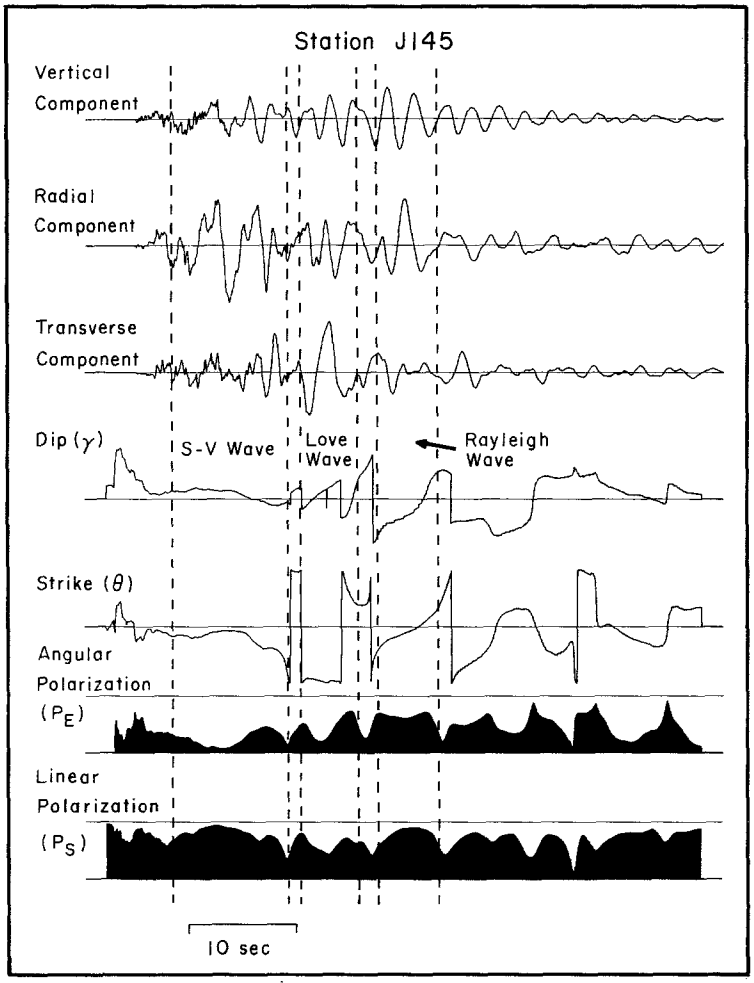


FIG. 5. Polarization analysis of the velocity records from station J145. Three arrivals are identified: an $S$ wave; a Love wave; and a Rayleigh wave. The strike ($\theta$), dip ($\delta$), angular polarization ($P_E$), and linear polarization ($P_S$) are defined in the text. A time window of 3 sec is used.

The earlier arrival of the Rayleigh wave may occur because it samples deeper and faster rock than the Love wave. These Rayleigh and Love waves can be well explained with the two-dimensional structure from Duke *et al.* (1971) outlined in the lower panel of Figure 3. Figure 8 shows the result of the finite difference modeling from Vidale and Helmberger (1986b) for the station S267. The source depth and mechanism are derived from previous teleseismic studies. The polarization of the energy justifies the use of the two-dimensional rather than fully three-dimensional finite difference method, and the finite difference method can explain most of the long-period strong motions.

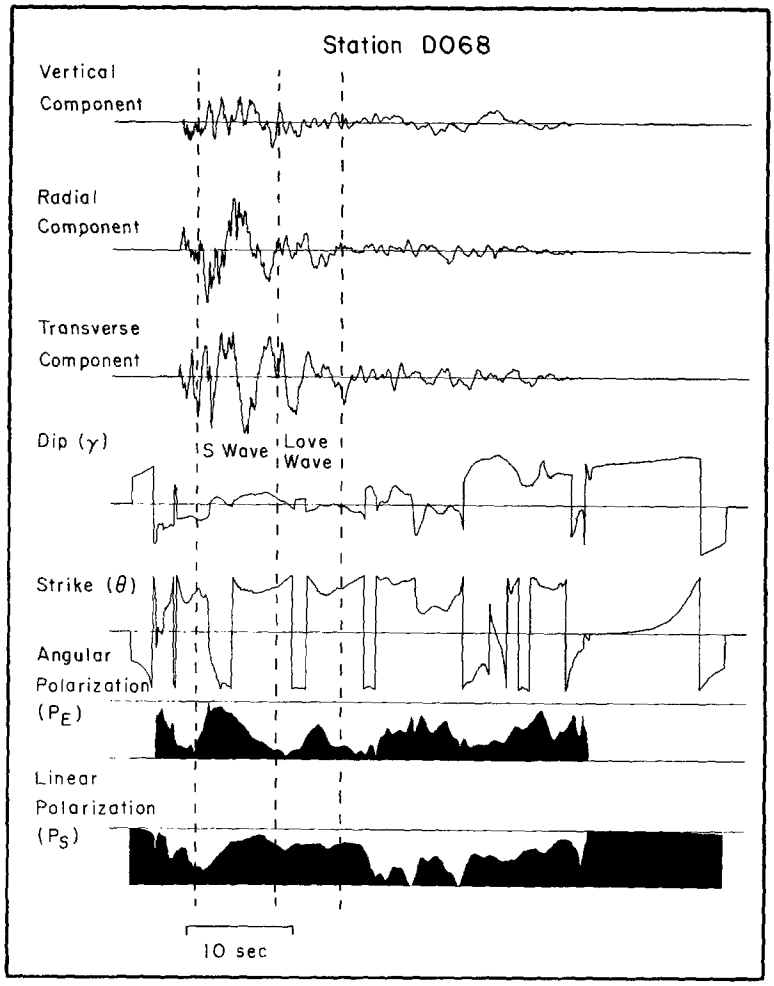


FIG. 6. Polarization analysis of the velocity records from station D068. Two arrivals are identified: an $S$ wave and a Love wave. A Rayleigh wave is also tentatively identified. The strike ($\theta$), dip ($\delta$), angular polarization ($P_E$), and linear polarization ($P_S$) are defined in the text. A time window of 3 sec is used.

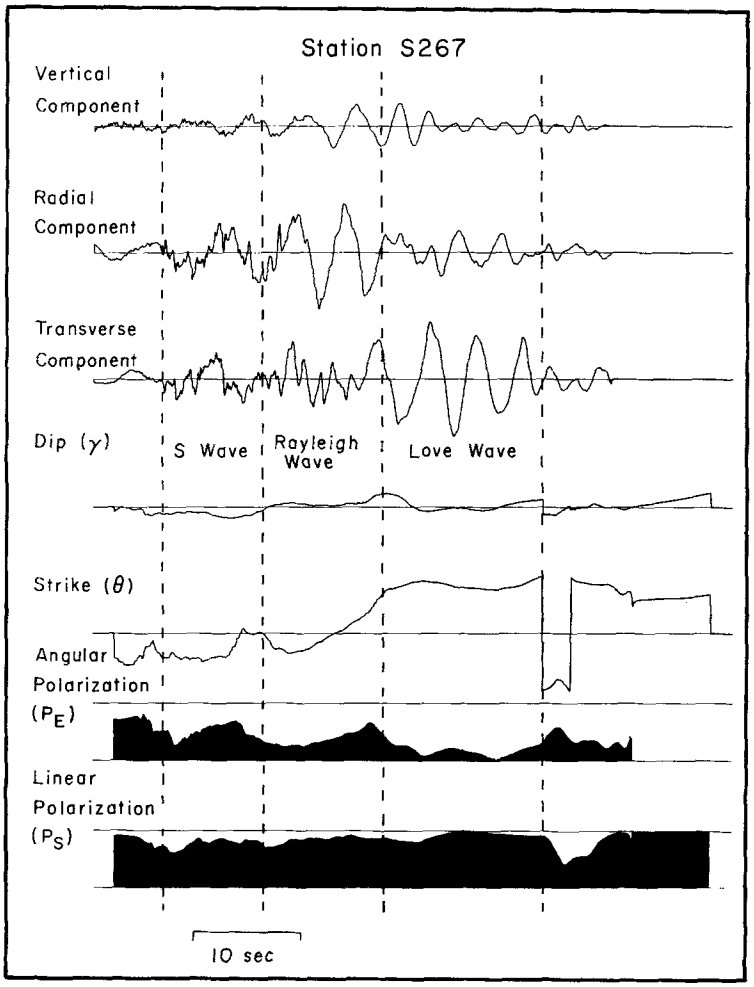


FIG. 7. Polarization analysis of the velocity records from station S267. Three arrivals are identified: an $S$ wave; a Love wave; and a Rayleigh wave. The strike ($\theta$), dip ($\delta$), angular polarization ($P_E$), and linear polarization ($P_S$) are defined in the text. A time window of 3 sec is used.

By identifying the arrivals with the use of complex polarization filter and then modeling those arrivals with forward finite difference calculations (in Vidale and Helmberger, 1986b), the observations shown in Figure 4 can be explained. Body waves and surface waves generated near the hypocenter propagate across the San Fernando basin with the expected travel times. At the Santa Monica Mountains, the surface waves are destroyed by the lateral heterogeneity in structure. The observed Love and Rayleigh waves in the Los Angeles basin are created by the conversion of *S* body waves to surface waves near the edge of the Los Angeles basin. This analysis is supported by the observation that body waves tend to convert to surface waves when they are incident on the near edge of a basin (see, e.g., Figure 14 in Vidale *et al.*, 1985).

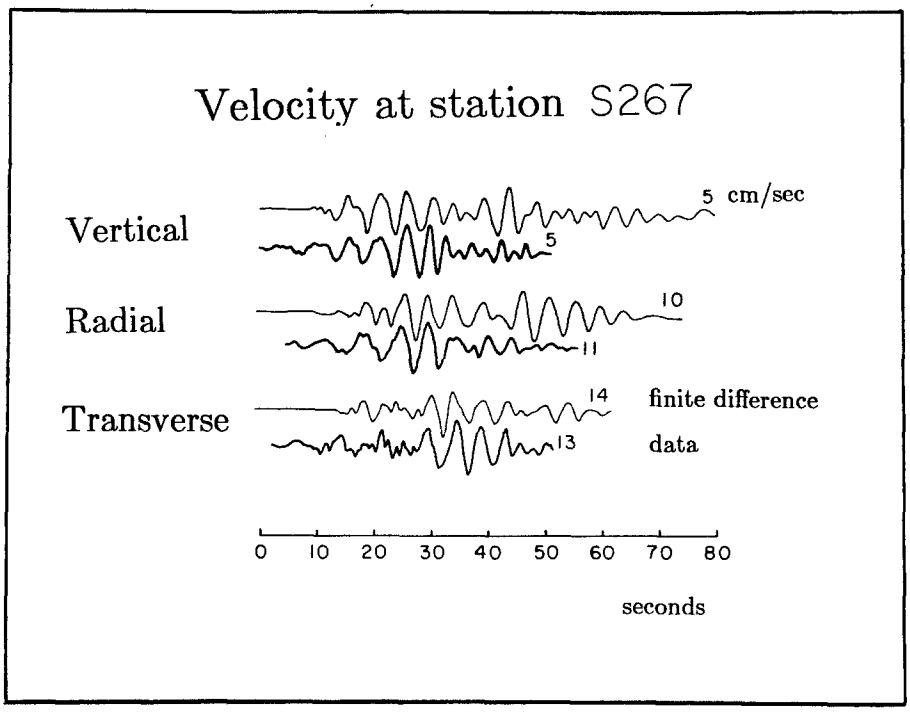


FIG. 8. Comparison of the data (heavy traces) with the finite difference seismograms (light lines) from Vidale and Helmberger (1986b) for station S267. The polarization identification of the Love and Rayleigh waves is supported by the finite difference modeling, which predicts Love and Rayleigh waves at the times that they actually arrive. The amplitudes and waveforms match well between the data and the finite difference seismograms.

## CONCLUSIONS

The complex polarization filter described in this paper allows routine analysis of three-component seismograms to yield the wave type of arrivals. This analysis is shown to aid in the interpretation of strong motions recorded in and around the basins in Los Angeles. In combination with finite difference forward modeling, this analysis suggests that *S* body waves that convert to surface waves on striking basin structures supply the energy that enables the basins to shake longer than the surrounding mountains.

## ACKNOWLEDGMENTS

This work was partly supported by Air Force-Cambridge Grant F19628-83-K-0010 and NSF Grant CEE-8121719. J. E. V. was supported by an NSF fellowship. Donald V. Helmberger gave valuable advice, and critical reviews by Heidi Houston, Don L. Anderson, Richard Stead, and an anonymous reviewer were helpful. Contribution number 4300 from the Division of Geological and Planetary Sciences, California Institute of Technology.

## REFERENCES

Aki, K. and P. G. Richards (1980). *Quantitative Seismology, Theory and Methods*, W. H. Freeman and Co., San Francisco, California, 768 pp.

Duke, C. M., J. A. Johnson, Y. Kharraz, K. W. Campbell, and N. A. Malpiede (1971). Subsurface site conditions and geology in the San Fernando earthquake area, UCLA-ENG-7206, School of Engineering, University of California at Los Angeles, Los Angeles, California.

Gal'perin, E. I. (1984). *The Polarization Method of Seismic Exploration*, Reidel Publishing Co., Boston, Massachusetts.

Haar, L., F. Vernon, J. Fletcher, E. Sembera, and J. Brune (1985). F-K spectra of body-wave coda from local earthquakes, *EOS* **66,** 954.

Kanasewich, E. R. (1981). *Time Sequence Analysis in Geophysics*, University of Alberta Press, Edmonton, Canada.

Kirkwood, S. C. and S. Crampin (1981). Surface-wave propagation in an ocean basin with an anisotropic upper mantle: observations of polarization anomalies, *Geophys. J. R. Astr. Soc.* **64,** 487–497.

Liu, H. L. and T. Heaton (1984). Array analysis of the ground velocities and accelerations from the 1971 San Fernando California earthquake, *Bull. Seism. Soc. Am.* **74,** 1951–1968.

Malvern, L. E. (1969). *Introduction to the Mechanics of a Continuous Medium*, Prentice-Hall, Inc., Englewood Cliffs, New Jersey.

Mims, C. H. and R. L. Sax (1965). Rectilinear motion direction (REMODE), Seismic Data Laboratory Report 118, Teledyne, Inc., Alexandria, Virginia (AD-460-631).

Montalbetti, J. R. and E. R. Kanasewich (1970). Enhancement of teleseismic body phases with a polarization filter, *Geophys. J. R. Astr. Soc.* **21,** 119–129.

Nuttli, O. (1961). The effect of the Earth's surface on the *S* wave particle motion, *Bull. Seism. Soc. Am.* **51,** 237–246.

Samson, J. C. and J. V. Olson (1980). Some comments on the description of polarization states of waves, *Geophys. J.* **21,** 115–129.

Smart, E. and H. Sproules (1981). Regional phase processors, VELA Seismological Center Report VSC-TR-81-19, Arlington, Virginia.

Trifunac, M. D., A. G. Brady, and D. E. Hudson (1973). Strong-motion earthquake accelerograms, corrected accelerograms and integrated ground velocity and displacement curves, vol. II, parts C, G, and J, Earthquake Engineering Research Laboratory, EERL 73-75, California Institute of Technology, Pasadena, California.

Vidale, J. E. and D. H. Helmberger (1986a). Path effects in strong motion seismology, *Methods of Computational Physics*, Bruce Bolt, Editor, Academic Press, Orlando, Florida (in press).

Vidale, J. E. and D. H. Helmberger (1986b). Elastic finite-difference modeling of the 1971 San Fernando, California earthquake (submitted for publication).

Vidale, J. E., D. V. Helmberger, and R. W. Clayton (1985). Finite-difference seismograms for *SH* waves, *Bull. Seism. Soc. Am.* **75,** 1765–1782.

SEISMOLOGICAL LABORATORY
CALIFORNIA INSTITUTE OF TECHNOLOGY
PASADENA, CALIFORNIA 91125

Manuscript received 16 January 1986